

Observation of antiferromagnetic fractons: Analysis of inelastic neutron scattering experiments

Takamichi Terao and Tsuneyoshi Nakayama

Department of Applied Physics, Hokkaido University, Sapporo 060-8628, Japan

(Received 28 May 2002; published 14 October 2002)

This paper presents an analysis of the experimental data obtained by means of inelastic neutron scattering (INS) experiments for diluted Heisenberg antiferromagnet $\text{RbMn}_{0.39}\text{Mg}_{0.61}\text{F}_3$. We have performed computer simulations in order to confirm the observations of antiferromagnetic fractons for this system. The profile of the dynamical structure factor $S(Q, \omega)$ has been calculated by applying the forced oscillator method, which is powerful for calculating the linear-response function of the antiferromagnetic system described by non-Hermitian matrices. Calculated results recover well INS results. These results confirm the observation of antiferromagnetic fractons in $\text{RbMn}_{0.39}\text{Mg}_{0.61}\text{F}_3$.

DOI: 10.1103/PhysRevB.66.132409

PACS number(s): 75.30.Ds, 75.40.Mg, 75.50.Ee

Critical dynamics of diluted magnets have been a subject of considerable interest in the contexts of statistical physics and physics of random systems.¹⁻³ Some classes of diluted Heisenberg magnets take the geometrical structures of percolating networks, which exhibit the typical random fractal structures.⁴⁻⁷ Diluted Heisenberg antiferromagnets do not belong to the same universal class as that for percolating elastics networks.⁸ This is because the equations of motion governing antiferromagnetic spin waves are not able to be mapped onto the equation of motion for elastic vibrations.⁹

Magnetic excitations in diluted antiferromagnetic systems have been theoretically investigated on the basis of the theory of fractons.¹⁰⁻¹⁵ The spin dynamics of the $d=3$ diluted Heisenberg antiferromagnet $\text{RbMn}_c\text{Mg}_{1-c}\text{F}_3$ has been extensively studied in terms of inelastic neutron scattering (INS) experiments by Ikeda and co-workers,¹⁶⁻¹⁸ where c is the concentration of the magnetic atoms in the system. They have investigated the energy spectra of magnetic excitations from the zone center to the zone boundary. A pure system of RbMnF_3 ($c=1$) has a cubic perovskite structure in which magnetic ions lie on a simple cubic lattice with the exchange interaction energy $J=0.29$ (meV). In a diluted system, the magnetic Mn^{2+} and nonmagnetic Mg^{2+} atoms are randomly arranged on the cubic lattice. This system belongs to an ideal isotropic Heisenberg antiferromagnet, because the magnitude of anisotropy is very small and the exchange interaction is dominant only for the nearest neighbors.¹⁶⁻¹⁸ The self-similarity becomes relevant at length scale shorter than a correlation length $\xi \approx a_0 |c - c_p|^{-\nu}$ (a_0 is the constant prefactor), where c and c_p are the percolation concentration and the percolation threshold, respectively. At larger length scale, the system is considered to be homogeneous, and the excitations on such structures exhibit a crossover at a length scale ξ . In diluted Heisenberg antiferromagnets, it is expected that propagating spin waves (magnons) with the wavelength larger than ξ cross over to antiferromagnetic fractons with shorter wavelength, which are strongly localized excitations reflecting the disorder and self-similarity of the system.⁹

With high concentration c , the magnetic excitation spectra are dominated by a sharp spin-wave peak in the small-wave-vector regime.¹⁶ In the large-wave-vector regime, the spectra show six well-resolved Ising-cluster excitations with a different number of neighbors ($1 \leq z \leq 6$), originating from the

different local environments in the diluted system. With $c=0.39$, Ikeda and co-workers^{17,18} have obtained the energy spectra at several wave vectors from $Q=0$ to $Q=0.375$ reciprocal lattice unit (rlu) (zone boundary). In Ref. 18, the peak intensity owing to magnons decreases with increasing wave number Q , and the definite magnon peak diminishes beyond $Q_c > Q$, where Q_c ($\sim 1/\xi$) is a crossover wave number.

We present in this paper numerical results of the dynamical structure factor $S(Q, \omega)$ on $d=3$ diluted Heisenberg antiferromagnets with the concentration $c=0.39$. The profile of $S(Q, \omega)$ recovers well the INS experiments in $\text{RbMn}_{0.39}\text{Mg}_{0.61}\text{F}_3$,¹⁸ where a magnon-fracton crossover is observed at the crossover energy ω_c . The localization nature of spin-wave excitations in diluted Heisenberg antiferromagnets near the percolation threshold ($c > c_p$) is numerically clarified by investigating the ω dependence of the participation number $\mathcal{P}(\omega)$. The calculated results indicate that the spin-wave excitations at $\omega \geq \omega_c$ are strongly localized, which is the characteristics of antiferromagnetic fracton excitations.

The Hamiltonian of diluted Heisenberg antiferromagnets is given by

$$\mathcal{H} = \sum_{\langle mn \rangle} J_{mn} \mathbf{S}_m \cdot \mathbf{S}_n, \quad (1)$$

where \mathbf{S}_m denotes the spin at the site m , and J_{mn} the exchange coupling between nearest-neighbor sites m and n . We choose J_{mn} as $J_{mn}=2J$ if sites m and n are connected, and $J_{mn}=0$ otherwise. The linearized equation of motion for spin deviation $S_i^+ \equiv S_i^x + iS_i^y$ is expressed by¹⁵

$$i \frac{\partial S_i^+}{\partial t} = \sigma_i \sum_j J_{ij} (S_i^+ + S_j^+). \quad (2)$$

Here σ_i is a variable taking $+1$ for the site i belonging to the up-spin sublattice and -1 to the down-spin sublattice. In Eq. (2), we take the unit of $S/\hbar=1$, and the magnitude of single spin S is given by $S=5/2$ for Mn atoms. In the following studies, we consider the spin dynamics of diluted Heisenberg antiferromagnets at low temperature, when the linearized spin-wave approximation is valid. Equation (2) is rewritten in the matrix form such as

$$\sum_j D_{ij} s_j(\lambda) = \omega_\lambda s_i(\lambda), \quad (3)$$

where $\{s_i(\lambda)\}$ is the eigenvector belonging to the eigenfrequency ω_λ , and the matrix element D_{ij} is defined by

$$D_{ij} = \sigma_i \left[J_{ij} + \delta_{ij} \sum_k J_{ik} \right]. \quad (4)$$

The physical properties of spin-wave excitations in diluted Heisenberg antiferromagnets can be clarified by analyzing the nonsymmetric dynamical matrix $\{D_{ij}\}$. It is mentioned that a nonsymmetric matrix has two sets of eigenvectors called right eigenvectors and left eigenvectors,¹⁴ and the spin-wave excitations corresponds to the right eigenvectors of the dynamical matrix D_{ij} [Eq. (3)].

Now we show numerical results for the dynamical structure factor $S(Q, \omega)$ on $d=3$ diluted Heisenberg antiferromagnets at the concentration $c=0.39$. The dynamical structure factor $S(Q, \omega)$ for antiferromagnetic spin waves is given by^{14,15,19}

$$S(Q, \omega) \propto \langle n+1 \rangle \chi''(Q, \omega) \propto \langle n+1 \rangle \sum_\lambda \delta(\omega - \omega_\lambda) \times \left\{ \sum_m e^{-i\mathbf{Q} \cdot \mathbf{R}_m} \sigma_m v_m(\lambda) \right\} \left\{ \sum_n e^{i\mathbf{Q} \cdot \mathbf{R}_n} u_n(\lambda) \right\}, \quad (5)$$

where $\langle n+1 \rangle$ is the Bose factor expressed by $1/(1 - e^{-\beta\omega})$, and $\chi''(Q, \omega)$ is the imaginary part of generalized susceptibility, \mathbf{R}_n is the positional vector of the site n , and σ_n is a variable taking $+1$ at the site n belonging to the up-spin sublattice or -1 for the down sublattice. In Eq. (5), $u_n(\lambda)$ and $v_n(\lambda)$ are the right and left eigenvectors of the dynamical matrix, respectively, describing the transverse spin deviations under the linearized spin-wave approximation.

We have numerically calculated the dynamical structure factor $S(Q, \omega)$ on diluted Heisenberg antiferromagnets at the percolation threshold ($c = c_p$), and demonstrated that antiferromagnetic fractons satisfy the single-length scaling postulate (SLSP).^{20,21} This implies that all length scales such as the wavelength, the localization length, and the scattering length collapse into a unique characteristic length scale $\Lambda(\omega)$. Namely, the dynamical structure factor $S(Q, \omega)$ for antiferromagnetic fractons is given by the following scaling form with the characteristic length $\Lambda(\omega)$ such as

$$S(Q, \omega) = Q^{-y} F[Q\Lambda(\omega)], \quad (6)$$

where $F(x)$ is a scaling function, and y is a new exponent characterizing $S(Q, \omega)$. We have also studied the dynamical structure factor $S(Q, \omega)$ with concentrations c close to c_p .¹⁵ Our results have shown that there is only one peak in the ω dependence of the dynamical structure factor at the magnon-fracton crossover with low concentration $c(>c_p)$. In Ref. 15, the dynamical structure factor with higher concentration shows the double-peak structure, reflecting the Ising-cluster excitations.²² The latter feature is in accord with the inelastic

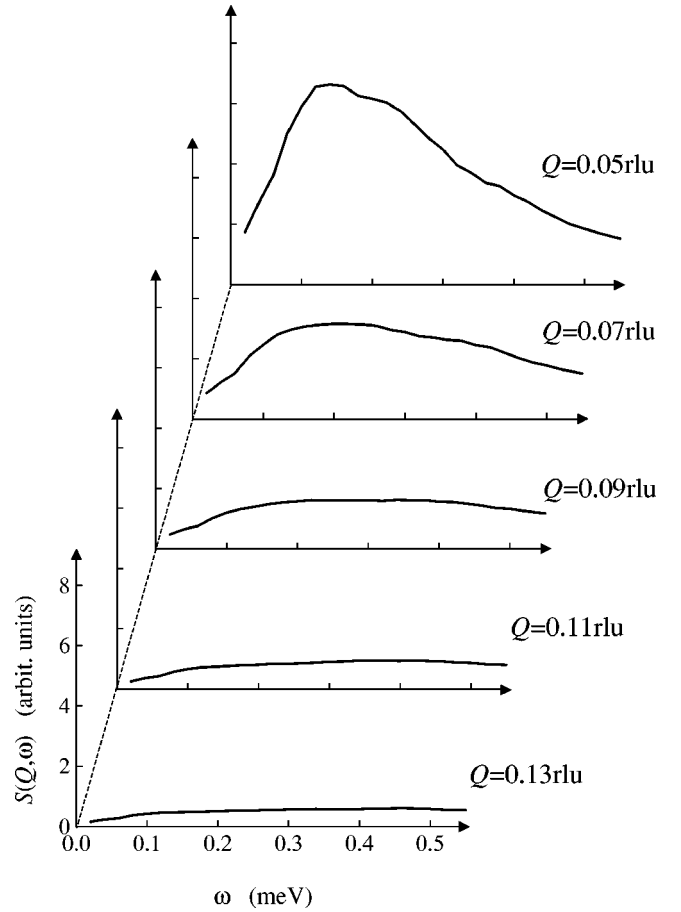


FIG. 1. The ω dependence of the dynamical structure factor $S(Q, \omega)$ with five different wave vectors Q . The concentration of the system is taken to be $c=0.39$.

neutron scattering experiments on $\text{RbMn}_c\text{Mg}_{1-c}\text{F}_3$ ($c = 0.74, 0.63$).¹⁶ The details of numerical methods are given in Refs. 14 and 23.

Figure 1 shows the ω dependence of $S(Q, \omega)$ for $d=3$ site-diluted antiferromagnets at $c=0.39$ ($c_p=0.312$) with five different wave vectors Q . The site-percolating network is formed on a $L \times L \times L$ cubic lattice, and periodic boundary conditions are employed in all spatial directions. In Fig. 1, we have calculated $S(Q, \omega)$ ($Q \equiv |\mathbf{Q}|$) with \mathbf{Q} along $[110]$ directions from the magnetic zone center. The magnitude of exchange interaction energy J and the energy resolution $\delta\omega$ are set to be $J=0.29$ (meV) and $\delta\omega \approx 0.02$ (meV), respectively. The ensemble average has been taken over four realizations of site-percolating networks formed on $60 \times 60 \times 60$ simple cubic lattice.²⁴ The largest network has 75 384 spins for $L=60$. Figure 1 indicates that the peak becomes broader, and the peak intensity diminishes at $Q > Q_c$ (≈ 0.1 rlu). We should mention that the direct comparison between Fig. 1 and experimental results¹⁸ is difficult, because the data in Fig. 3 in Ref. 18 include the background intensity in addition to the incoherent scattering component centered at $Q=0$ wavevector, and the spin-wave contribution is not separated from the observed spectrum. This is the reason for not making the direct comparison in Fig. 1 with the raw data given in Fig. 3 of Ref. 18. However, we see that the calculated results

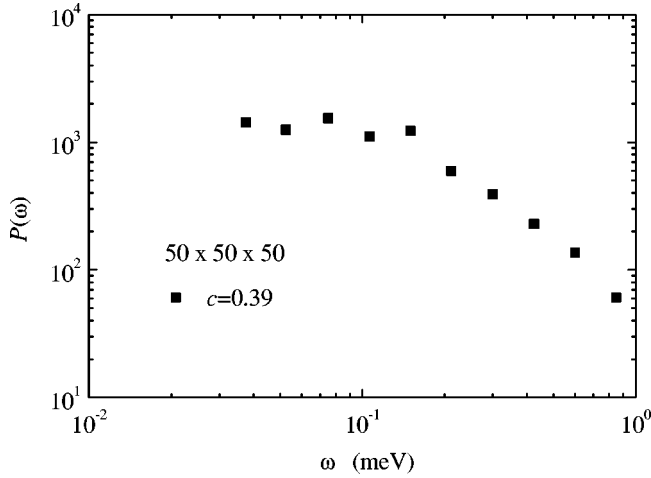


FIG. 2. The ω dependence of the participation number $\mathcal{P} = \mathcal{P}(\omega)$. The system size and the concentration are taken to be $L = 50$ and $c = 0.39$, respectively.

in Fig. 1 recover well the observed characteristics of dynamical structure factors $S(Q, \omega)$ presented in Ref. 18.

One of the important characteristics on the fracton excitation is its strongly localized nature.⁹ The localization nature of spin-wave excitations in diluted Heisenberg antiferromagnets is not fully clarified yet, and there is no direct calculation of the localization length of spin-wave excitations near the percolation threshold $c > c_p$. Here, we clarify the localized nature of spin-wave excitations on diluted Heisenberg antiferromagnets with $c > c_p$ by studying the ω dependence of participation number $\mathcal{P} = \mathcal{P}(\omega)$ at the magnon-fracton crossover numerically. The participation number $\mathcal{P}(\omega)$ is a quantity to clarify the localized nature of spin-wave excitations numerically. Using the eigenvectors $\{s_i(\lambda)\}$, the participation number $\mathcal{P}(\omega)$ is defined to be²⁵

$$\mathcal{P}(\omega) = \frac{\left\langle \left\{ \sum_i |s_i(\lambda)|^2 \right\}^2 \right\rangle_\omega}{\left\langle \sum_i |s_i(\lambda)|^4 \right\rangle_\omega}, \quad (7)$$

where $\langle \dots \rangle_\omega$ denotes the average over eigenmodes with frequencies close to ω . In general, the participation number $\mathcal{P}(\omega)$ is related to the localization length $\Lambda(\omega)$ of excitations, which is written as $\mathcal{P}(\omega) \sim c \{\Lambda(\omega)\}^d$ with the concentration c far from the critical concentration c_p (in the homogeneous system) or $\mathcal{P}(\omega) \sim \{\Lambda(\omega)\}^{D_f}$ with $c \approx c_p$ (in the self-similar system), where D_f is the fractal dimension of the system.

Using Eqs. (3), (4), and (7), we calculate the eigenvectors $\{s_i(\lambda)\}$ and the participation number $\mathcal{P}(\omega)$ for $d=3$ percolating Heisenberg antiferromagnets. The system size L and the concentration c are set to be $L=50$ and $c=0.39$, respectively, and the ensemble average is taken over 16 different samples. We obtain the eigenvectors of $\{D_{ij}\}$ in Eq. (4) by forced-oscillator method for nonsymmetric matrices.¹⁴ Figure 2 shows calculated results on the participation number $\mathcal{P} = \mathcal{P}(\omega)$. In Fig. 2, the abscissa and the ordinate denote the

energy of the spin-wave excitations ω in units of $J = 0.29$ (meV). It is shown that the value of $\mathcal{P}(\omega)$ becomes constant for lower energy regime [$\omega < 0.1$ (meV)], which is due to the finite-size effect of the system. This result implies that there is a propagating spin-wave excitations (magnons) in this energy regime. On the contrary, we see that $\mathcal{P}(\omega)$ decreases with increasing ω , indicating that the spin-wave excitations with $\text{RbMn}_{0.39}\text{Mg}_{0.61}\text{F}_3$ are localized for higher energy regimes [$\omega > 0.2$ (meV)]. From the scaling theory, the participation number $\mathcal{P}(\omega)$ and the localization length $\Lambda(\omega)$ in the self-similar regime are given by $\mathcal{P}(\omega) \sim \{\Lambda(\omega)\}^{D_f}$ and $\Lambda(\omega) \sim \omega^{-\tilde{d}/D_f}$, respectively, where \tilde{d} is the spectral dimension. This indicates that the participation number $\mathcal{P}(\omega)$ shows the power-law behavior such as $\mathcal{P}(\omega) \sim \omega^{-\tilde{d}}$, where the value of the spectral dimension \tilde{d} is known to be $\tilde{d} \approx 1$ for antiferromagnetic fractons.^{8,20} In Fig. 2, our calculated results for higher energy regime agree well with the theoretical prediction on $\mathcal{P}(\omega)$. These results support the existence of a crossover from magnons to fracton excitations in $\text{RbMn}_{0.39}\text{Mg}_{0.61}\text{F}_3$.¹⁸

Christou and Stinchcombe have obtained an analytic expression of $S(Q, \omega)$ of percolating antiferromagnets in the long-wavelength limit $Q\xi \ll 1$, which satisfies the dynamical scaling hypothesis.²⁶ Their result shows that the dynamical structure factor $S(Q, \omega; \xi)$ becomes

$$S(Q, \omega; \xi) = \frac{A Q^{-2z} (Q\xi)^d}{\{\omega Q^{-z} - (Q\xi)^{1-z}\}^2 + (Q\xi)^{2(1+d-z)}} \quad (8)$$

near the percolation threshold ($c > c_p$), where d and z are the Euclidean dimension and the dynamical exponent, respectively. In Eq. (8), there is a sharp peak on the ω dependence of $S(Q, \omega; \xi)$ with the wavenumber $Q < Q_c$, where $Q_c \sim 1/\xi$ is the crossover wave number. This contribution comes from magnons at the lower energy regime in diluted Heisenberg antiferromagnets. The peak intensity rapidly decreases with increasing the wavenumber Q , and this peak due to spin-wave excitations becomes very broad and overdamped at $Q \sim Q_c$. Our calculated results shows a good agreement with the essential feature in Eq. (8) as well as the INS experiments.¹⁸

In conclusion, we have investigated the dynamical properties of spin-wave excitations in $d=3$ diluted Heisenberg antiferromagnets $\text{RbMn}_{0.39}\text{Mg}_{0.61}\text{F}_3$. The calculated results of $S(Q, \omega)$ have indicated that the sharp magnon peak is observed at $Q < Q_c$ (≈ 0.1 rlu), and its peak disappears at $Q > Q_c$. The profile of ω dependence on the calculated results recovers well the INS experiments, where a magnon-fracton crossover is observed in $\text{RbMn}_{0.39}\text{Mg}_{0.61}\text{F}_3$.¹⁸ We have also calculated the ω dependence of the participation number $\mathcal{P}(\omega)$ to clarify the localization nature of spin-wave excitations in diluted Heisenberg antiferromagnets. The ω dependence of the participation number $\mathcal{P}(\omega)$ on diluted Heisenberg antiferromagnets has been studied numerically beyond the percolation threshold. From the calculated results of $\mathcal{P}(\omega)$, it is shown that the spin-wave excitations with $\omega < \omega_c$ is propagating beyond the system size L . With

$\omega > \omega_c$, on the contrary, the ω dependence of $\mathcal{P}(\omega)$ decreases with higher energy regimes. This indicates that the spin-waves with $\omega > \omega_c$ are strongly localized, which is the characteristic feature of antiferromagnetic fracton excitations. These results have confirmed that the experiments in Ref. 18 have truly observed the existence of antiferromagnetic fractons in diluted Heisenberg antiferromagnets $\text{RbMn}_{0.39}\text{Mg}_{0.61}\text{F}_3$.

One of the authors (T.N.) is indebted to stimulating conversations with the late Hironobu Ikeda, who had been one of pioneers of neutron scattering experiments for diluted magnets. This work was supported in part by a Grant-in-Aid from the Japan Ministry of Education, Science, and Culture for Scientific Research. The authors thank the Supercomputer Center, Institute of Solid State Physics, University of Tokyo for the use of the facilities.

-
- ¹A. B. Harris and S. Kirkpatrick, Phys. Rev. B **16**, 542 (1977).
²E. F. Shender, Zh. Eksp. Teor. Fiz. **75**, 352 (1978) [Sov. Phys. JETP **48**, 175 (1978)].
³D. Kumar and A. B. Harris, Phys. Rev. B **32**, 3251 (1985).
⁴J. Campo, F. Palacio, C. C. Becerra, A. R. Wildes, L. P. Regnault, and J. E. Lorenzo Diaz, J. Magn. Magn. Mater. **226-230**, 479 (2001).
⁵S. N. Kaul and S. Srinath, Phys. Rev. B **63**, 094410 (2001).
⁶M. Mekata, K. M. Kojima, I. Watanabe, K. Nagamine, and H. Ikeda, Physica B **289**, 194 (2000).
⁷H. Ikeda and K. Ohoyama, Phys. Rev. B **45**, 7484 (1992).
⁸T. Nakayama, K. Yakubo, and R. Orbach, Rev. Mod. Phys. **66**, 381 (1994).
⁹S. Alexander and R. Orbach, J. Phys. (France) Lett. **43**, L625 (1982).
¹⁰R. Orbach and K.-W. Yu, J. Appl. Phys. **61**, 3689 (1987).
¹¹G. Polatsek, O. Entin-Wohlman, and R. Orbach, Phys. Rev. B **39**, 9353 (1989).
¹²K. Yakubo, T. Terao, and T. Nakayama, J. Phys. Soc. Jpn. **62**, 2196 (1993).
¹³K. Yakubo, T. Terao, and T. Nakayama, J. Phys. Soc. Jpn. **63**, 3431 (1994).
¹⁴T. Terao, K. Yakubo, and T. Nakayama, Phys. Rev. E **50**, 566 (1994).
¹⁵T. Terao and T. Nakayama, Phys. Rev. B **51**, 11 479 (1995).
¹⁶M. Takahashi and H. Ikeda, Phys. Rev. B **47**, 9132 (1993).
¹⁷H. Ikeda, J. A. Fernandez-Baca, R. M. Nicklow, M. Takahashi, and K. Iwasa, J. Phys.: Condens. Matter **6**, 10543 (1994).
¹⁸H. Ikeda, S. Itoh, M. A. Adams, and J. A. Fernandez-Baca, J. Phys. Soc. Jpn. **67**, 3376 (1998).
¹⁹W. Marshall and S. W. Lovesey, *Theory of Thermal Neutron Scattering: The Use of Neutrons for the Investigation of Condensed Matter* (Clarendon Press, Oxford, 1971).
²⁰T. Terao, K. Yakubo, and T. Nakayama, Phys. Rev. B **49**, 12 281 (1994).
²¹S. Alexander, E. Courtens, and R. Vacher, Physica A **195**, 286 (1993).
²²S. Kirkpatrick and T. P. Eggater, Phys. Rev. B **6**, 3598 (1972).
²³T. Nakayama and K. Yakubo, Phys. Rep. **349**, 238 (2001).
²⁴D. Stauffer and A. Aharony, *Introduction to Percolation Theory*, 2nd ed. (Taylor & Francis, London, 1992).
²⁵D. J. Thouless, Phys. Rep., Phys. Lett. **13C**, 93 (1974).
²⁶A. Christou and R. B. Stinchcombe, J. Phys. C **19**, 5917 (1986).